

Preparation, physical properties and n-type FET characteristics of substituted diindenopyrazinediones and bis(dicyanomethylene) derivatives†‡

Jun-ichi Nishida,* Hironori Deno, Satoru Ichimura, Tomohiro Nakagawa and Yoshiro Yamashita*

Received 3rd October 2011, Accepted 22nd November 2011

DOI: 10.1039/c2jm14955a

A series of halogen and alkyl substituted diindenopyrazinediones and bis(dicyanomethylene) derivatives have been synthesized as new n-type organic semiconductors based on nitrogen-containing heterocycles. Halogen groups were introduced to improve the electron injection. Their crystal structures and solid physical properties are discussed. Alkyl groups were introduced to increase the solubility in organic solvents. Furthermore, hexanoyl groups were introduced by oxidation of alkyl groups to increase the solubility and electron affinity. Dicyanomethylene groups were also introduced to further enhance the electron-accepting properties. Drop-cast as well as vapour deposited thin films showed n-type FET properties.

Introduction

Organic field-effect transistors (OFETs) have attracted much attention in recent years owing to advantages such as large-area fabrication and mechanical flexibility leading to their possible applications in electronic devices.¹ Development of new organic semiconductors is very important for progress in this field. Compared with hole-transporting materials, the numbers of n-type materials are still limited and their development is strongly required.² As a promising approach to obtain new

n-type organic semiconductors, nitrogen-containing heterocycles are used as important components to construct the π -units.³ They can be prepared by a simple reaction and have strong electron-accepting properties with planar geometries. Introduction of nitrogen-heterocycles such as pyrazine,⁴ thiazole,⁵ pyrimidine,⁶ and benzothiadiazole⁷ provides high performance n-type semiconductors as well as stable p-type semiconductors.^{8,9} Recently, indenofluorenone derivatives **1** have attracted attention as a core unit affording n-type semiconductors.^{10,11} We have replaced the central benzene ring with pyrazine to give diindenopyrazine derivatives **2a,b**.¹¹ Compared with indenofluorenediones, they have lower LUMO levels (*ca.* 0.3 eV) than **1**.¹¹ As a result, **2a** exhibited n-type FET performances in contrast to **1a** (R=H) which showed no FET behaviour. Introduction of fluoro substituents improved FET performances and the derivative **2b** showed a high electron mobility of 0.17 cm² V⁻¹ s⁻¹ and a low threshold voltage of +17 V.¹¹ As an extension of this work, chloro and bromo derivatives were also prepared and their crystal structures and solid physical properties are discussed here. On the other hand, the halogen substituted derivatives **2a–d** are hardly dissolved in organic solvents. To improve the solubility, alkyl substituted derivatives **2e** and **2f** have now been prepared. Furthermore, acyl substituents and dicyanomethylene groups were introduced to increase the electron-accepting properties. We report their preparation, physical properties and FET characteristics (Fig. 1).

Results and discussion

Synthesis and characterization

Chloro and bromo substituted diindenopyrazinediones **2c** and **2d** were prepared for comparisons with **2a,b**. Alkyl substituted diindenopyrazinediones **2e** and **2f** were also synthesized by

Department of Electronic Chemistry, Interdisciplinary Graduate School of Science and Engineering, Tokyo Institute of Technology, 4259 Nagatsuta, Midori-ku, Yokohama, 226-8502, Japan. E-mail: yoshiro@echem.titech.ac.jp; Fax: +81-45-924-5489; Tel: +81-45-924-5571

† Electronic supplementary information (ESI) available: UV-Vis spectra, FET characteristics, XRD data and AFM images. CCDC reference numbers 846545 and 846546. For ESI and crystallographic data in CIF or other electronic format see DOI: 10.1039/c2jm14955a.

‡ X-Ray measurement of single crystals of **2c** and **2d** was carried out using a RAXIS-RAPID imaging plate diffractometer with Mo-K α radiation ($\lambda = 0.71075$ Å) at -180.0 °C. The structure was solved by the direct method (SIR2004) and refined by the full-matrix least-squares method on F^2 . The non-hydrogen atoms were refined anisotropically. Hydrogen atoms were refined using the riding model. Absorption correction was applied using an empirical procedure. All calculations were performed using the CrystalStructure crystallographic software package except for refinement, which was performed using SHELXL-97. *Crystal data for 2c*: C₁₈H₆Cl₂N₂O₂, $M = 353.16$, red block, crystal dimensions $0.50 \times 0.30 \times 0.10$ mm, monoclinic, space group $P2_1/n$, $a = 6.73$ (1), $b = 7.65$ (2), $c = 13.37$ (2) Å, $\beta = 94.23$ (6) °, $V = 687$ (2) Å³, $Z = 2$, $D_c = 1.708$ g cm⁻³, 6347 reflections collected, 1560 independent ($R_{\text{int}} = 0.0761$), GOF = 1.064, $R_1 = 0.0572$ ($I > 2.00 \sigma(I)$), $wR_2 = 0.1448$ for all reflections. *Crystal data for 2d*: C₁₈H₆Br₂N₂O₂, $M = 442.07$, red block, crystal dimensions $0.20 \times 0.10 \times 0.05$ mm, monoclinic, space group $P2_1/n$, $a = 6.838$ (8), $b = 7.76$ (1), $c = 13.38$ (2) Å, $\beta = 92.92$ (5) °, $V = 709$ (2) Å³, $Z = 2$, $D_c = 2.070$ g cm⁻³, 6693 reflections collected, 1624 independent ($R_{\text{int}} = 0.0877$), GOF = 0.873, $R_1 = 0.0364$ ($I > 2.00 \sigma(I)$), $wR_2 = 0.0650$ for all reflections. The CCDC reference numbers are 846545 and 846546.

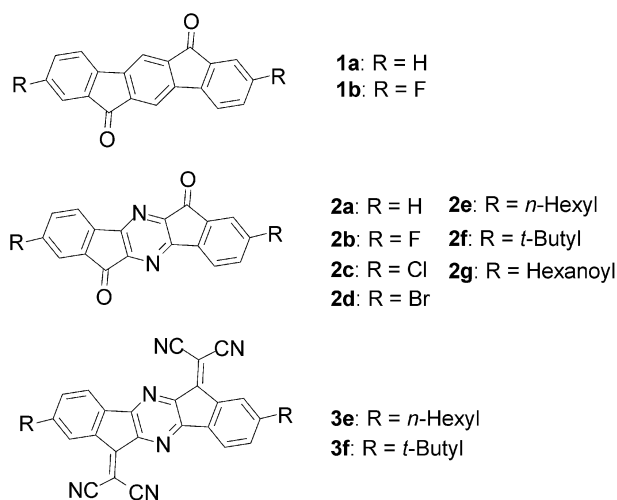
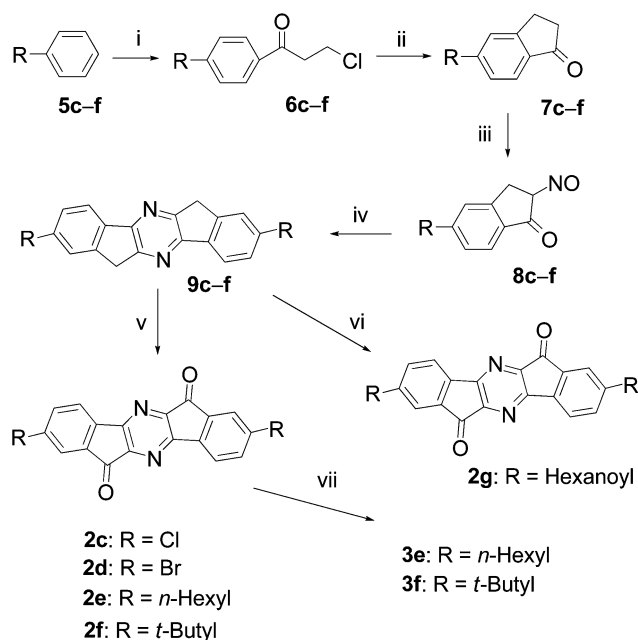


Fig. 1 Chemical structures of indenofluorendiones **1**, diindenopyrazinediones **2** and bis(dicyanomethylene) derivatives **3**.

a similar method as **2a**.¹² The procedure is shown in Scheme 1. Hexanoyl substituted derivative **2g** was synthesized by oxidation reaction of intermediate **9e** with an excess amount of sodium dichromate in 19% yield. Since **2g** is dissolved in organic solvents, purification was carried out by using column chromatography and sublimation. Bis(dicyanomethylene) derivatives **3** were prepared by condensation reaction with malononitrile in DMSO in a microwave reactor. Since hexyl derivative **3e** was not dissolved in organic solvents, *tert*-butyl derivative **3f** was also prepared. These compounds were purified by sublimation.



Scheme 1 Synthetic procedures of diindenopyrazinedione derivatives. *Reagents:* (i) AlCl₃, CH₂Cl₂; (ii) conc. H₂SO₄; (iii) isoamyl nitrite, conc. HCl, benzene; (iv) Na₂S₂O₄, EtOH, NH₃ aq.; (v) Na₂Cr₂O₇, AcOH, Ac₂O; (vi) Na₂Cr₂O₇, AcOH, Ac₂O; (vii) CH₂(CN)₂, DMSO.

X-Ray crystal structure analysis

X-Ray single crystal analysis of halogen substituted compounds **2b**,¹¹ **2c** and **2d** was carried out to investigate the intermolecular interactions (Fig. 2). These compounds are completely planar and form π -stacking structures. Fluoro derivative **2b** shows a polymorphism and afforded two kinds of crystals, black and red ones. These were prepared by multiple sublimation. The overlap patterns of molecules are different as shown in Fig. 2a and b. In the black crystal, the whole molecule is involved with close contacts between the carbon of the carbonyl group and the oxygen of adjacent molecules, whereas in the red crystal, only a half of the molecule is overlapped with close contacts between the carbon of the carbonyl group and the halogens of adjacent molecules (3.21 Å). Chlorine and bromine derivatives **2c** and **2d** afforded only red crystals with similar carbonyl and halogen contacts (**2c**: 3.37 Å, **2d**: 3.44 Å) and the same space group ($P2_1/n$) as depicted in Fig. 2c and d. Interplanar distances are different depending on the halogen size (**2b** red: 3.22 Å, **2c**: 3.36 Å, **2d**: 3.42 Å).

Photophysical properties

The compounds prepared here are almost colourless in solution. UV-Vis spectra of the alkyl substituted compounds are described in Fig. 3. In compound **2e** with hexyl groups, the absorption maxima were observed at 325 and 376 nm and a weak intramolecular charge-transfer (CT) band was observed at 476 nm. The weak CT band is blue-shifted in **2g** with hexanoyl groups (Fig. S1, ESI[†]). On the other hand, bis(dicyanomethylene) derivatives **3e** and **3f** showed red-shifted end-absorptions in dichloromethane or DMF.

In contrast to the solution spectra, in the solid state, these compounds showed dark colours (**2b**: black and red, **2c**: red, **2d**: red, **2e**: dark red, **2g**: orange and **3e**: green). Reflection spectra in the solid state were measured by using an integrated sphere and the spectra were transformed to the corresponding absorption spectra (K - M transformation) (Fig. 4). The difference in the crystal colour is obvious in Fig. 4a. An end-absorption of red crystals is observed at 600 nm, whereas that of the black crystal is red-shifted to 700 nm. This large shift (100 nm) provides a small HOMO-LUMO energy gap. On the other hand, the solid colour

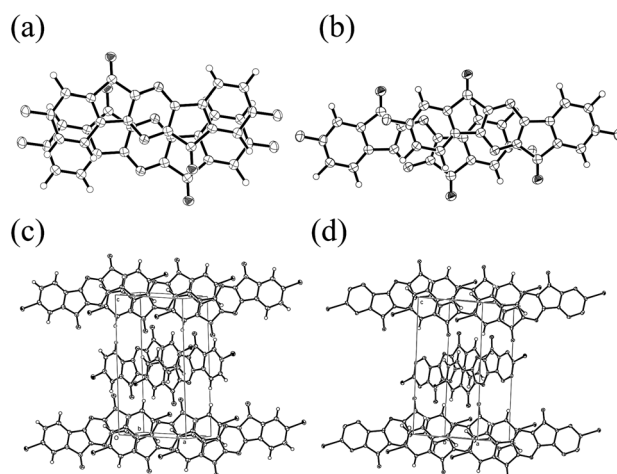


Fig. 2 Overlap modes in (a) black and (b) red crystals of **2b**. Crystal structures of (c) **2c** and (d) **2d**.

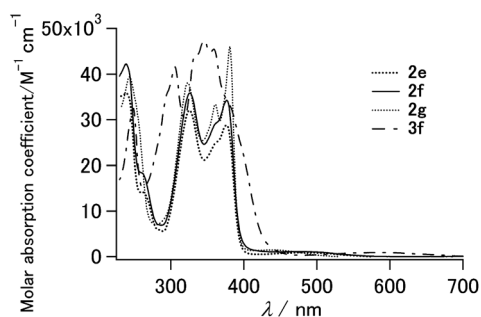


Fig. 3 UV-Vis spectra of indenopyrazinedione derivatives **2e**, **2f** and **2g** and bis(dicyanomethylene) derivatives **3f** in CH_2Cl_2 .

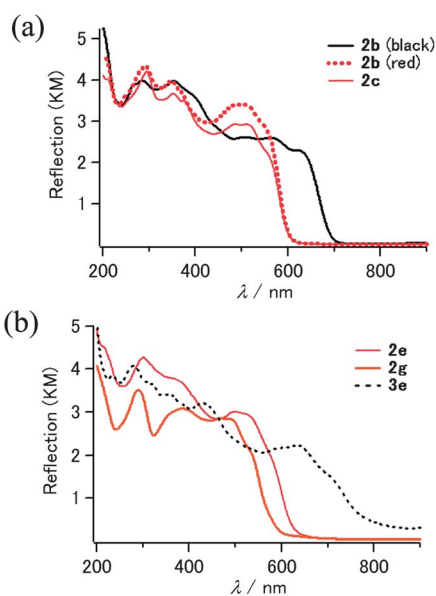


Fig. 4 Reflection spectra of compounds (a) **2b** (black and red solids) and **2c** and (b) **2e**, **2g** and **3e** in solid state after K-M transformation.

reflects the molecular arrangements. In turn, replacement of hexyl groups with hexanoyl groups in **2g** afforded a blue-shift of the end-absorption as shown in Fig. 4b. Since the blue-shift was also observed in the solution spectra (Fig. 3), the shift is considered to be related to an intramolecular charge transfer (CT) band. A large red-shift of the end-absorption was observed in **3e** with strong electron-withdrawing groups. These results may be explained by considering the intra- and intermolecular CTs from the outside benzene ring to the pyrazine core.

Electrochemical properties

Compounds **2** and **3** have electron-accepting properties attributed to the pyrazine and fused cyclopentadienone units. Their reduction potentials were measured by cyclic voltammetry (CV) and the results are summarized in Table 1. In hexyl substituted compound **2e**, two reversible reduction peaks were observed as shown in Fig. 5a. The introduction of hexanoyl groups in **2g** led to 0.2 V positive shifts of the reduction potentials. *tert*-Butyl substituted compound **2f** showed similar reduction potentials as **2e**. While bis(dicyanomethylene) derivative **3e** was not dissolved in any solvents, the reduction potentials of *tert*-butyl derivative **3f** were

measured as shown in Fig. 5b. The HOMOs and LUMOs are estimated by the DFT calculations based on the B3LYP/6-31G(d) level (Fig. 6) (calculated HOMO of **2e**: 6.11 eV, **2g**: 6.71 eV, **3e**: 6.46 eV; LUMO of **2e**: 3.09 eV, **2g**: 3.54 eV, **3e**: 4.01 eV).

FET characteristics

The FET devices based on compounds **2** and **3** were fabricated on SiO_2/Si wafers by vapour-deposition with bottom contact geometry. The SiO_2 gate dielectric surface was treated with hexamethyldisilazane (HMDS). The FET measurements were carried out at room temperature in a high vacuum chamber (10^{-5} Pa). The FET performances are summarized in Table 2. Chloro and bromo substituted derivatives **2c,d** showed lower electron mobilities than the fluoro derivative **2b**. This may be attributed to the longer interplanar distances in π -stacks of **2c,d** as revealed by X-ray analysis. Compound **2e** with hexyl groups showed an electron mobility of $1.6 \times 10^{-5} \text{ cm}^2 \text{ V}^{-1} \text{ s}^{-1}$, when the wafer was kept at 100°C . Introduction of hexanoyl groups improved the mobility to $9.2 \times 10^{-3} \text{ cm}^2 \text{ V}^{-1} \text{ s}^{-1}$ in **2g**, which is 500 times higher than that of **2e**. The mobility was almost similar to that of the fluorine derivative **2b**. This result suggests that terminal carbonyl groups are effective in increasing electron mobility. Introduction of bis(dicyanomethylene) groups also improved the electron mobility in compound **3e**. The highest mobility of $1.1 \times 10^{-2} \text{ cm}^2 \text{ V}^{-1} \text{ s}^{-1}$ was obtained (Fig. 7). After exposure to air, FETs based on **2g** gradually deteriorated. The air-stability was improved in dicyanomethylene compounds **3**. Thus, compound **3e** exhibited an electron mobility of $1.7 \times 10^{-3} \text{ cm}^2 \text{ V}^{-1} \text{ s}^{-1}$ and a high on/off ratio (10^5) in air (after 3 h). The stability can be ascribed to the lower LUMO level and the high crystallinity of the thin film (*vide infra*).

Since some of these compounds can be dissolved in organic solvents, a drop-cast method was applied for fabrication of FETs. After chloroform solutions of **2g** and **3f** were drop-cast on a channel, the devices were annealed at 100°C *in vacuo* for 20 min. Their films showed n-type FET characteristics and the results are summarized in Table 3. The film **2g** on an untreated surface afforded an electron mobility of $1.7 \times 10^{-5} \text{ cm}^2 \text{ V}^{-1} \text{ s}^{-1}$ and the film **3f** exhibited a mobility of $5.3 \times 10^{-5} \text{ cm}^2 \text{ V}^{-1} \text{ s}^{-1}$. The low mobility in **2g** compared with those of vapour-deposited films in Table 2 may be ascribed to the large grain boundary as detected by atomic force microscopy (AFM), which is caused by the large grains with vertical interval maxima of *ca.* 73 nm on the untreated surface and *ca.* 116 nm on the HMDS treated surface (Fig. S1–S4 in ESI†). The low mobility in **3f** may be attributed to the amorphous-type structures.

XRD analysis and AFM measurements

The thin films of **2** and **3** were examined by X-ray diffraction (XRD) in reflection mode. The XRD patterns of films are shown in Fig. 8. In the thin film **2e**, a sharp first reflection was observed at $2\theta = 4.8^\circ$ (*d*-space: 18.3 Å), when the SiO_2/Si wafer was kept at room temperature. When the wafer was kept at 100°C , a new peak was observed at 5.5° (*d*-space: 16.1 Å), indicating the presence of two patterns of molecular arrangements in the film. Since the calculated molecular length of **2e** is 26.7 Å, the molecules are considered to take declined orientation or telescope-type arrangements. In the film **2g**, similar first reflection peaks

Table 1 Optical and electrochemical data

Compd	$\lambda_{\text{abs}}/\text{nm}$ (log ϵ)	E_{pc}/V^c	LUMO ^e
2a	268, 317, 367, 455 ^a	-0.52, -1.08 ^{ac}	3.85
2b	267, 311, 361, 469 ^a	-0.41, -0.99 ^{ac}	3.96
2c	267, 316, 356, 372, 456 ^a	- ^d	- ^d
2d	267, 319, 357, 374, 416 ^a	- ^d	- ^d
2e	239 (4.55), 326 (4.51), 376 (4.46), 476 (2.95) ^b	-0.63, -1.07 ^{bc}	3.74
2f	239 (4.62), 326 (4.55), 377 (4.53) ^b	-0.62 ^{bc}	3.75
2g	244 (4.60), 323 (4.58), 381 (4.66), 440 (3.16) ^b	-0.43, -0.90 ^{bc}	3.93
3e	249, 305, 346, 358, 581 ^a	- ^d	- ^d
3f	249 (4.51), 306 (4.62), 346 (4.68) ^b	-0.22, -0.56 ^{bc}	4.15

^a In DMF. ^b In CH₂Cl₂. ^c 0.1 M *n*-Bu₄NPF₆, Pt electrode, *V* vs. SCE. Half-wave potentials. ^d Low solubility. ^e Calculated from reduction potentials.

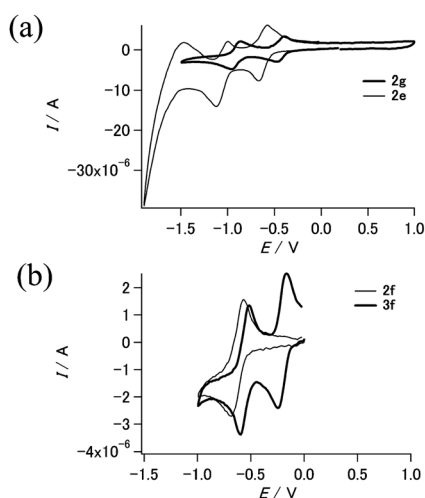


Fig. 5 Cyclic voltammograms of (a) compounds **2e** and **2g** and (b) *tert*-butyl substituted **2f** and **3f**.

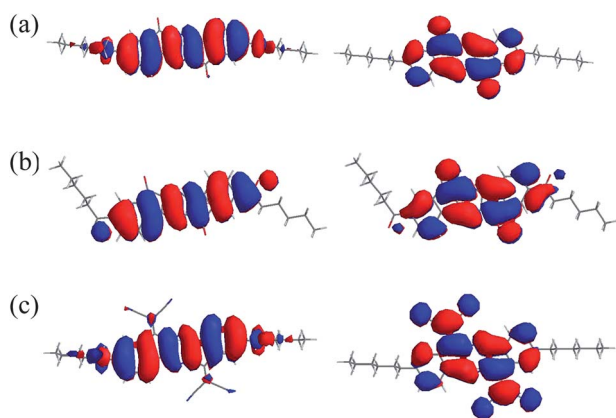


Fig. 6 DFT calculations of HOMOs (left) and LUMOs (right) of (a) **2e**, (b) **2g** and (c) **3e**.

were observed at 4.6° at room temperature and 5.1° at 100 °C. In the drop-cast film **2g**, the first reflection peak was observed at 5.2° (*d*-space: 16.1 Å) accompanied by two other peaks. In the case of bis(dicyanomethylene) derivative **3e**, a sharp reflection peak was observed at 5.6° (*d*-space: 15.6 Å), and the peak did not change against the surface conditions and the substrate temperatures. Since the molecular length is 27.5 Å, the molecules are

considered to have an *ca.* 35° declining orientation on the substrate. In contrast to the reflection peaks, the FET properties were dependent on the surface conditions and temperatures.

To further study the film morphology, the surface of the thin film **3e** was investigated by using atomic force microscopy (AFM) with the tapping mode. As the substrate temperature increased up to 100 °C, the grain size and grain boundaries became larger (Fig. 9). The large grain boundary is considered to result in the decrease of the mobility at high substrate temperatures.

Conclusions

In summary, we have developed new halogen and alkyl substituted diindenopyrazinediones and the bis(dicyanomethylene) derivatives, and applied them to FETs. Halogen groups were effective in enhancing the electron-accepting abilities of the compounds and improved the FET performances. On the other hand, alkyl groups were effective in enhancing the solubility in organic solvents. Introduction of hexanoyl groups increased the electron affinity leading to improved FET properties. Bis(dicyanomethylene) derivatives showed strong electron-accepting properties and the FETs exhibited air stability. Further modifications of the electron-accepting π -units and terminal groups are under way.

Experimental

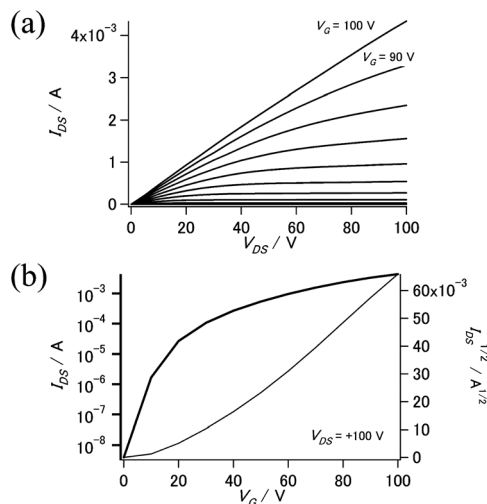
General information

Melting points were obtained using a SHIMADZU DSC-60. ¹H-NMR spectra were recorded on a JEOL JNM-ECP 300 spectrometer. DI-MS data were collected on a JEOL JMS-700 mass spectrometer. IR spectra were recorded using a JASCO FT/IR-4100 Fourier Transform Infrared Spectrometer. UV-Vis spectra were recorded on a JASCO V-650 spectrophotometer. Reflection spectra in the solid states were collected using a JASCO ISV-722 integrated sphere. Cyclic voltammograms and differential pulse voltammograms were recorded on a HOKUTODENKO HZ-5000. Pt disk, Pt wire and SCE were used as working, counter, and reference electrodes. Tetrabutylammonium hexafluorophosphate (TBAPF₆; 0.1 mol dm⁻³) was used as a supporting electrolyte in dry DMF or dichloromethane. MO calculations were carried out by DFT methods at the B3LYP/6-31G(d) level using the Gaussian program 03. X-Ray diffraction (XRD) measurements were carried out on a Rigaku RINT with

Table 2 FET characteristics based on vapour deposited films^a

Compd	Surface	T_{sub} (degree)	Mobility/($\text{cm}^2 \text{V}^{-1} \text{s}^{-1}$)	On/off	Threshold/V
2b (black) ^b	HMDS	20	1.1×10^{-2}	1×10^6	+27
2b (red) ^b	HMDS	20	8.7×10^{-3}	9×10^5	+27
2c	HMDS	20	2.2×10^{-4}	8×10^5	+35
2d	HMDS	20	1.4×10^{-6}	2×10^2	+14
2e	HMDS	20	1.1×10^{-6}	2×10^2	+52
	HMDS	100	1.6×10^{-5}	2×10^3	+25
2f	HMDS	20	7.4×10^{-8}	9×10	+15
2g	Bare	20	4.3×10^{-4}	8×10^5	+21
	HMDS	20	1.3×10^{-3}	1×10^6	+36
	Bare	60	9.4×10^{-4}	1×10^6	+36
	HMDS	60	5.6×10^{-3}	1×10^6	+45
	Bare	100	9.2×10^{-3}	2×10^6	+46
	HMDS	100	1.1×10^{-3}	1×10^6	+17
3e	Bare	20	1.1×10^{-2}	1×10^6	+25
	HMDS	20	2.7×10^{-3}	1×10^4	+20
	Bare	100	4.6×10^{-5}	3×10^3	+6
	HMDS	100	3.3×10^{-4}	3×10^3	+16
3f	HMDS	20	1.2×10^{-4}	1×10^4	+31

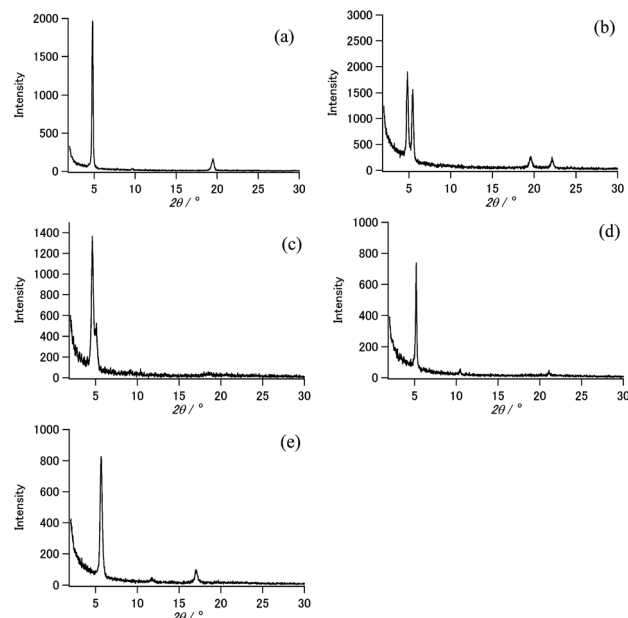
^a Bottom contact configuration. ^b Ref. 11. Polymorphism.

**Fig. 7** (a) Output and (b) transfer characteristics of FET **3e**.

a $\text{CuK}\alpha$ source ($\lambda = 1.541 \text{ \AA}$). AFM experiments for films in a tapping mode were performed using a SII NanoTechnology SPA-400 (DFM) instrument.

Materials

3-Chloro-1-(4-hexylphenyl)propanone (6e). To a suspension of AlCl_3 (9.07 g, 68.0 mmol) in dry CH_2Cl_2 (20 mL), a solution of 3-chloropropionylchloride (9.77 g, 76.9 mmol) in CH_2Cl_2

**Fig. 8** X-Ray diffractograms of films of (a) **2e** at $T_{\text{sub}} = 20 \text{ }^\circ\text{C}$ on untreated surface, (b) **2e** at $100 \text{ }^\circ\text{C}$ on HMDS treated surface, (c) **2g** at $20 \text{ }^\circ\text{C}$ on HMDS treated surface, (d) **2g** deposited by drop-cast method on untreated surface, and (e) **3e** at $20 \text{ }^\circ\text{C}$ on untreated surface.

(10 mL) was added slowly. After the reaction mixture was stirred for 15 min at room temperature, a solution of hexylbenzene (**5e**) (10.2 g, 62.9 mmol) in CH_2Cl_2 (10 mL) was added slowly, and the

Table 3 FET characteristics based on the solution process^a

Compd	Method	Surface	Mobility/ $\text{cm}^2 \text{V}^{-1} \text{s}^{-1}$	On/off	Threshold/V
2g	Solution	Bare	1.7×10^{-5}	8×10^2	+36
	Solution	HMDS	2.9×10^{-6}	1×10^2	+22
3f	Solution	Bare	3.9×10^{-5}	5×10	>0
	Solution	HMDS	5.3×10^{-5}	1×10^2	>0

^a Bottom contact configuration.

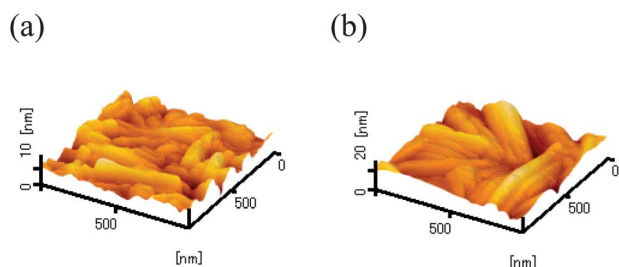


Fig. 9 AFM images of films of **3e** at $T_{\text{sub}} =$ (a) 20 °C and (b) 100 °C on untreated SiO₂ surfaces.

resulting mixture was stirred for 24 h at room temperature. The mixture was poured onto ice, and was extracted with CH₂Cl₂. The organic layer was washed with aq. NaHCO₃ and brine, and dried over Na₂SO₄. The organic solvent was removed, and the crude product was purified by column chromatography (SiO₂: CH₂Cl₂) to give a colourless solid of **6e** (15.8 g, 99%).

¹H-NMR (300 MHz; CDCl₃): δ 7.89 (dd, $J = 8.1, 1.8$ Hz, 2H), 7.28 (dd, $J = 8.1, 1.8$ Hz, 2H), 3.92 (t, $J = 7.5$ Hz, 2H), 3.45 (t, $J = 7.5$ Hz, 2H), 2.67 (t, $J = 7.8$ Hz, 2H), 1.58–1.68 (m, 2H), 1.27–1.35 (m, 6H), 0.88 (t, $J = 7.2$, 3H).

5-Hexyl-1-indanone (7e). A mixture of **6e** (4.38 g, 17.3 mmol) and conc. H₂SO₄ (60 mL) was stirred at 120 °C for 2 h. The resulting mixture was poured onto ice and was extracted with CH₂Cl₂. The organic layer was neutralized with aq. NaHCO₃, washed with brine and dried over Na₂SO₄. After the organic solvent was removed, the crude product was purified by column chromatography (SiO₂: CH₂Cl₂) to give yellow oil of **7e** (2.24 g, 60%).

¹H-NMR (CDCl₃): δ 7.67 (d, $J = 7.8$ Hz, 1H), 7.39 (s, 1H), 7.19 (d, $J = 7.8$ Hz, 1H), 3.11 (t, $J = 5.4$ Hz, 2H), 2.71–2.66 (m, 4H), 1.66–1.60 (m, 2H), 1.32–1.31 (m, 6H), 0.89 (br. t, 3H).

5-Hexyl-2-nitroso-1-indanone (8e). To a solution of **7e** (987 mg, 4.56 mmol) in benzene (6 mL), a solution of isoamyl nitrite (558 mg, 4.76 mmol) in conc. HCl (2 mL) was added dropwise at 40 °C. The reaction mixture was stirred at 40 °C for 3 h and 3 d at room temperature. The reaction mixture was extracted with CH₂Cl₂, and the organic layer was neutralized with aq. NaHCO₃, washed with brine, and dried over Na₂SO₄. Purification by SiO₂ column chromatography (eluent: CH₂Cl₂/ethyl acetate) gave a colourless solid of **8e** (670 mg, 60%).

¹H-NMR (DMSO): δ 7.66 (d, $J = 8.1$ Hz, 1H), 7.45 (br. s, 1H), 7.31 (br. d, $J = 8.1$ Hz, 1H), 3.74 (s, 2H), 2.69 (t, $J = 7.2$ Hz, 2H), 1.62–1.58 (m, 2H), 1.35–1.25 (m, 6H), 0.86 (t, $J = 7.2$ Hz, 3H).

2,8-Dihexyldiindeno[1,2-*b*;1',2'-*e*]pyrazine (9e). A mixture of **8e** (3.05 g, 12.4 mmol), sodium dithionite (7.24 g, 41.6 mmol), ethanol (13 mL) and aq. NH₃ (28%, 26 mL) was refluxed for 24 h under Ar. The reaction mixture was extracted with CH₂Cl₂, and the organic layer was washed with brine, and dried over Na₂SO₄. Purification by SiO₂ column chromatography (eluent: CH₂Cl₂) gave a colorless solid of **9e** (532 mg, 20%).

Mp: 185.2–188.3 °C. ¹H-NMR (CDCl₃): δ 8.01 (d, $J = 8.1$ Hz, 2H), 7.45 (s, 2H), 7.32 (d, $J = 8.1$ Hz, 2H), 4.02 (s, 4H), 2.72 (t, $J = 7.5$ Hz, 4H), 1.70–1.63 (m, 4H), 1.35–1.31 (m, 12H), 0.89 (t, $J = 6.3$ Hz, 6H). IR (KBr) ν (cm⁻¹): 2999, 2928, 2852, 1618, 1466, 1362, 1243, 1162, 1119, 826, 656, 431.

2,8-Di-*tert*-butyldiindeno[1,2-*b*;1',2'-*e*]pyrazine (9f). A mixture of 5-*tert*-butyl-2-nitroso-1-indanone (**8f**)¹³ (3.02 g, 13.9 mmol), sodium dithionite (7.57 g, 57.9 mmol), ethanol (13 mL) and aq. NH₃ (28%, 26 mL) was refluxed for 24 h under Ar. The reaction mixture was extracted with CH₂Cl₂, and the organic layer was washed with brine, and dried over Na₂SO₄. Purification by SiO₂ column chromatography (eluent: CH₂Cl₂) gave a colorless solid of **9f** (591 mg, 23%).

Mp: 304.2–308.5 °C. ¹H-NMR (CDCl₃): δ 8.04 (d, $J = 8.4$ Hz, 2H), 7.68 (s, 2H), 7.56 (dd, $J = 8.4, 2.1$ Hz, 2H), 4.05 (s, 4H), 1.40 (s, 18H). IR (KBr) ν (cm⁻¹): 3073, 2950, 2921, 1616, 1457, 1370, 1248, 1136, 1126, 831, 663, 434.

2,8-Dihexyldiindeno[1,2-*b*;1',2'-*e*]pyrazine-6,12-dione (2e). A mixture of **9e** (140 mg, 0.33 mmol), Na₂Cr₂O₇/2H₂O (290 mg, 0.97 mmol), acetic acid (9 mL) and acetic anhydride (1 mL) was refluxed under Ar for 24 h. After addition of water at room temperature, the resulting precipitate was collected by suction. Purification by SiO₂ column chromatography (eluent: CH₂Cl₂) followed by sublimation gave a red solid of **2e** (35.4 mg, 24%).

Mp: >271 °C (sublimation). ¹H-NMR (CDCl₃): δ 7.88 (d, $J = 8.1$ Hz, 2H), 7.65 (br. s, 1H), 7.50 (br. d, $J = 8.1$ Hz, 2H), 2.70 (t, $J = 7.5$ Hz, 4H), 1.70–1.60 (m, 4H), 1.35–1.25 (m, 12H), 0.93–0.85 (br. t, 6H). IR (KBr) ν (cm⁻¹): 2953, 2924, 2855, 1726, 1605, 1463, 1382, 1216, 1154, 1131, 418. MS/FAB: m/z 453 (M⁺ + 1). Anal. Calcd for C₃₀H₃₂N₂O₂: C, 79.61; H, 7.13; N, 6.19. Found: C, 79.38; H, 7.23; N, 6.01%.

2,8-Di-*tert*-butyldiindeno[1,2-*b*;1',2'-*e*]pyrazine-6,12-dione (2f). A mixture of **9f** (997 mg, 2.71 mmol), Na₂Cr₂O₇/2H₂O (2.42 g, 8.12 mmol), acetic acid (50 mL) and acetic anhydride (5 mL) was refluxed under Ar for 24 h. After addition of water at room temperature, the resulting precipitate was collected by suction. Purification of the crude product by SiO₂ column chromatography (eluent: CH₂Cl₂) gave a red solid of **2f** (246 mg, 23%).

Mp: 366.5–368.2 °C. ¹H-NMR (CDCl₃): δ 7.91 (d, $J = 8.1$ Hz, 2H), 7.89 (d, $J = 2.1$ Hz, 2H), 7.73 (dd, $J = 8.1, 2.1$ Hz, 2H), 1.39 (s, 18H). IR (KBr) ν (cm⁻¹): 2958, 2867, 1736, 1608, 1473, 1454, 1364, 1215, 1176, 1151, 839, 430. MS/FAB: m/z 397 (M⁺ + 1). Anal. Calcd for C₂₆H₂₄N₂O₂: C, 78.76; H, 6.10; N, 7.07. Found: C, 78.45; H, 6.00; N, 6.97%.

2,8-Dihexanoyldiindeno[1,2-*b*;1',2'-*e*]pyrazine-6,12-dione (2g). A mixture of **9e** (291 mg, 0.68 mmol), Na₂Cr₂O₇/2H₂O (2.05 g, 6.86 mmol), acetic acid (25 mL) and acetic anhydride (5 mL) was stirred at 40 °C for 3 d. After addition of water and aq. NaHCO₃, the resulting precipitate was collected by suction. Purification by SiO₂ column chromatography (eluent: CH₂Cl₂) followed by sublimation gave a reddish-orange solid of **2g** (67.4 mg, 20%).

Mp: >310 °C (sublimation). ¹H-NMR (CDCl₃): δ 8.41 (br. s, 2H), 8.37 (br. d, $J = 7.8$ Hz, 2H), 8.15 (d, $J = 7.8$ Hz, 2H), 3.02 (t, $J = 7.2$ Hz, 4H), 1.80–1.75 (m, 4H), 1.45–1.35 (m, 12H), 0.93 (br. t, 6H). IR (KBr) ν (cm⁻¹): 3093, 2932, 2864, 1731, 1685, 1606, 1500, 1213, 1159, 1140, 1108, 437. MS/EI (70 eV): m/z 409 (M⁺ – C₅H₁₁, 100), 480 (M⁺, 19). Anal. Calcd for C₃₀H₂₈N₂O₄: C, 74.98; H, 5.87; N, 5.83. Found: C, 74.93; H, 5.73; N, 5.84%.

2,2'-(2,8-Dihexyldiindeno[1,2-*b*;1',2'-*e*]pyrazine-6,12-diylidene)dimalononitrile (3e). A mixture of **2e** (96.6 mg, 0.21 mmol),

malononitrile (164 mg, 2.48 mmol) and DMSO (10 mL) was stirred in a microwave reactor (350 W) for 90 s. After addition of water at room temperature, the resulting precipitate was collected by suction. Purification of crude product by sublimation afforded a dark green solid of **3e** (28.1 mg, 24%).

Mp: >276 °C (sublimation). MS/EI (70 eV): *m/z* 548 (M^+ , 100). Anal. Calcd for $C_{36}H_{32}N_6$: C, 78.80; H, 5.88; N, 15.32. Found: C, 78.96; H, 6.06; N, 15.10%. IR (KBr) ν (cm^{-1}): 2950, 2927, 2847, 2229, 1463, 1245, 1174, 1136, 850.

2,2'-(2,8-Di-tert-butyl-diindenol[1,2-*b*;1',2'-*e*]pyrazine-6,12-diyli-dene)dimalononitrile (3f). A mixture of **2f** (246 mg, 0.620 mmol), malononitrile (456 mg, 6.91 mmol) and DMSO (15 mL) was stirred in a microwave reactor (350 W) for 90 s. After addition of water at room temperature, the resulting precipitate was collected by suction. Purification of the crude product by SiO_2 column chromatography (eluents: CH_2Cl_2 : toluene = 1 : 1) gave a red solid of **3f** (126 mg, 41%).

Mp: 360.6–363.8 °C. 1H -NMR ($CDCl_3$): δ 8.26 (s, 2H), 7.92 (br. d, 2H), 7.82 (br. d, 2H), 1.35 (s, 18H). IR (KBr) ν (cm^{-1}): 2967, 2872, 2225, 1615, 1581, 1478, 1368, 1233, 1166, 848. MS/FAB: *m/z* 493 ($M^+ + 1$). Anal. Calcd for $C_{32}H_{24}N_6$: C, 78.03; H, 4.91; N, 17.06. Found: C, 78.04; H, 4.78; N, 17.08%.

2,8-Dichlorodiindenol[1,2-*b*;1',2'-*e*]pyrazine (9c). Chlorinated compound **9c** was prepared by a cyclization reaction similar to that of 5-chloro-2-nitroso-1-indanone (**8c**)¹⁴ with sodium dithionite and purified by sublimation.

9c: colorless solid (63% yield), mp: >346.5 (sublimation), 1H -NMR ($CDCl_3$): δ 8.04 (d, $J = 8.4$ Hz, 2H), 7.64 (s, 2H), 7.49 (br. d, $J = 8.4$ Hz, 2H), 4.06 (s, 4H).

2,8-Dichlorodiindenol[1,2-*b*;1',2'-*e*]pyrazine-6,12-dione (2c). Compound **2c** was prepared by an oxidation reaction similar to that of **9c** with $Na_2Cr_2O_7/2H_2O$ and purified by sublimation.

2c: a red solid (49% yield), mp: >403.3 °C (sublimation). MS/EI (70 eV): *m/z* 352 (M^+ , 100). Anal. Calcd for $C_{18}H_6Cl_2N_2O_2$: C, 61.22; H, 1.71; N, 7.93. Found: C, 61.10; H, 1.52; N, 7.95%.

2,8-Dibromodiindenol[1,2-*b*;1',2'-*e*]pyrazine-6,12-dione (2d). Brominated compound **2d** was prepared by an oxidation reaction similar to that of dibromodiindenol[1,2-*b*;1',2'-*e*]pyrazine (**9d**)¹⁵ with $Na_2Cr_2O_7/2H_2O$ and purified by sublimation.

2d: a red solid (66% yield), mp: >450 °C. MS/EI (70 eV): *m/z* 442 (M^+ , 100). Anal. Calcd for $C_{18}H_6Br_2N_2O_2$: C, 48.91; H, 1.37; N, 6.34. Found: C, 48.81; H, 1.23; N, 6.37%.

Device fabrication

Bottom-contact FET. Highly doped n^+ -Si wafers were used as substrates, and a layer of 300 nm of silicon dioxide (SiO_2 : grown by thermal oxidation) was used as a gate dielectric layer. Cr (10 nm)/Au (20 nm) was successively evaporated and photolithographically delineated to obtain source and drain electrodes. The interdigitated structure of the source–drain contacts determined a channel length of 25 μm and a channel width of 294 μm (6 mm \times 49). Substrates were cleaned with acetone, 2-propanol and ozone for 20 min, and immersed in hexamethyldisilazane

(HMDS) at rt for 12 h to treat the surface. Organic semiconductor layers (500 Å) were deposited on the channel region by vacuum evaporation at a rate of 0.2–0.3 Å s^{-1} under a pressure of 10^{-5} Pa.

Mobilities (μ) were calculated in the saturation regime by the relationship: $\mu_{sat} = (2I_{DSL})/[WC_{ox}(V_G - V_{th})^2]$ where I_{DS} is the source–drain saturation current. C_{ox} is the oxide capacitance. V_G is the gate voltage and V_{th} is the threshold voltage. The latter can be estimated as the intercept of the linear section of the plot of $(I_{DS})^{1/2}$ vs. V_G .

Acknowledgements

This work was supported by a Grant-in-Aid for Scientific Research (no. 19350092 and 22550162) from the Ministry of Education, Culture, Sports, Science and Technology, Japan, and by the Global COE program “Education and Research Center for Emergence of New Molecular Chemistry”. We thank the Center for Advanced Materials Analysis, Technical Department, TIT for measurements of elemental analysis and MS.

Notes and references

- (a) H. E. Katz, A. J. Lovinger and J. G. Laquindanum, *Chem. Mater.*, 1998, **10**, 457; (b) M. Halik, H. Klauk, U. Zschieschang, G. Schmid, S. Ponomarenko, S. Kirchmeyer and W. Weber, *Adv. Mater.*, 2003, **15**, 917; (c) T. Sekitani, Y. Noguchi, K. Hata, T. Fukushima, T. Aida and T. Someya, *Science*, 2008, **321**, 1468.
- (a) H. Usta, C. Risko, Z. Wang, H. Huang, M. K. Delimeroglu, A. Zhukhovitskiy, A. Facchetti and T. J. Marks, *J. Am. Chem. Soc.*, 2009, **131**, 5586; (b) A. R. Murphy and J. M. J. Fréchet, *Chem. Rev.*, 2007, **108**, 1066; (c) C. R. Newman, C. D. Frisbie, D. A. da Silva Filho, J. L. Brédas, P. C. Ewbank and K. R. Mann, *Chem. Mater.*, 2004, **16**, 4436; (d) Y. Sun, Y. Liu and D. Zhu, *J. Mater. Chem.*, 2005, **15**, 53.
- (a) B. J. Jung, N. J. Tremblay, M.-L. Yeh and H. E. Katz, *Chem. Mater.*, 2011, **23**, 568; (b) S. Miao, A. L. Appleton, N. Berger, S. Barlow, S. R. Marder, K. I. Hardcastle and U. H. F. Bunz, *Chem.–Eur. J.*, 2009, **15**, 4990; (c) Y.-Y. Liu, C.-L. Song, W.-J. Zeng, K.-G. Zhou, Z.-F. Shi, C.-B. Ma, F. Yang, H.-L. Zhang and X. Gong, *J. Am. Chem. Soc.*, 2010, **132**, 16349; (d) Y. Fujisaki, Y. Nakajima, D. Kumaki, T. Yamamoto, S. Tokito, T. Kono, J.-i. Nishida and Y. Yamashita, *Appl. Phys. Lett.*, 2010, **97**, 133303; (e) Y. Zhu, R. D. Champion and S. A. Jenekhe, *Macromolecules*, 2006, **39**, 8712; (f) A. L. Briseno, F. S. Kim, A. Babel, Y. Xia and S. A. Jenekhe, *J. Mater. Chem.*, 2011, **21**, 16461.
- (a) Z. Liang, Q. Tang, J. Xu and Q. Miao, *Adv. Mater.*, 2011, **23**, 1535; (b) Naraso, J.-i. Nishida, D. Kumaki, S. Tokito and Y. Yamashita, *J. Am. Chem. Soc.*, 2006, **128**, 9598; (c) T. Kojima, J.-i. Nishida, S. Tokito, H. Tada and Y. Yamashita, *Chem. Commun.*, 2007, 1430; (d) H. Wang, Y. Wen, X. Yang, Y. Wang, W. Zhou, S. Zhang, X. Zhan, Y. Liu, Z. Shuai and D. Zhu, *ACS Appl. Mater. Interfaces*, 2009, **1**, 1122.
- (a) S. Ando, R. Murakami, J. Nishida, H. Tada, Y. Inoue, S. Tokito and Y. Yamashita, *J. Am. Chem. Soc.*, 2005, **127**, 14996; (b) M. Mamada, J.-i. Nishida, D. Kumaki, S. Tokito and Y. Yamashita, *Chem. Mater.*, 2007, **19**, 5404; (c) Y. Ie, M. Nitani, M. Karakawa, H. Tada and Y. Aso, *Adv. Funct. Mater.*, 2010, **20**, 907.
- T. Kojima, J.-i. Nishida, S. Tokito and Y. Yamashita, *Chem. Lett.*, 2009, **38**, 428.
- (a) J. Zaumseil, C. L. Donley, J.-S. Kim, R. H. Friend and H. Sirringhaus, *Adv. Mater.*, 2006, **18**, 2708; (b) T. Kono, D. Kumaki, J.-i. Nishida, T. Sakanoue, M. Kakita, H. Tada, S. Tokito and Y. Yamashita, *Chem. Mater.*, 2007, **19**, 1218.
- (a) Q. Miao, T.-Q. Nguyen, T. Someya, G. B. Blanchet and C. Nuckolls, *J. Am. Chem. Soc.*, 2003, **125**, 10284; (b) Naraso, J.-i. Nishida, S. Ando, J. Yamaguchi, K. Itaka, H. Koinuma, H. Tada, S. Tokito and Y. Yamashita, *J. Am. Chem. Soc.*, 2005,

- 127, 10142; (c) E. Ahmed, A. L. Briseno, Y. Xia and S. A. Jenekhe, *J. Am. Chem. Soc.*, 2008, **130**, 1118.
- 9 (a) T. Yamamoto, H. Kokubo, M. Kobashi and Y. Sakai, *Chem. Mater.*, 2004, **16**, 4616; (b) I. Osaka, R. Zhang, J. Liu, D.-M. Smilgies, T. Kowalewski and R. D. McCullough, *Chem. Mater.*, 2010, **22**, 4191; (c) H. N. Tsao, D. M. Cho, I. Park, M. R. Hansen, A. Mavrinskiy, D. Y. Yoon, R. Graf, W. Pisula, H. W. Spiess and K. Müllen, *J. Am. Chem. Soc.*, 2011, **133**, 2605.
- 10 (a) H. Usta, A. Facchetti and T. J. Marks, *J. Am. Chem. Soc.*, 2008, **130**, 8580; (b) Y. Miyata, T. Minari, T. Nemoto, S. Isoda and K. Komatsu, *Org. Biomol. Chem.*, 2007, **5**, 2592; (c) S. Merlet, M. Birau and Z. Y. Wang, *Org. Lett.*, 2002, **13**, 2157; (d) D. Vak, B. Lim, S. Lee and D. Kim, *Org. Lett.*, 2005, **19**, 4229; (e) Y.-I. Park, J. S. Lee, B. J. Kim, B. Kim, J. Lee, D. H. Kim, S.-Y. Oh, J. H. Cho and J.-W. Park, *Chem. Mater.*, 2011, **23**, 4038.
- 11 T. Nakagawa, D. Kumaki, J.-i. Nishida, S. Tokito and Y. Yamashita, *Chem. Mater.*, 2008, **20**, 2615.
- 12 F. Ebel and W. Deuschel, *Chem. Ber.*, 1956, **89**, 2799.
- 13 A. Gomtsyan, E. K. Bayburt, R. G. Schmidt, C. S. Surowy, P. Honore, K. C. Marsh, S. M. Hannick, H. A. McDonald, J. M. Wetter, J. P. Sullivan, M. F. Jarvis, C. R. Faltynek and C.-H. Lee, *J. Med. Chem.*, 2008, **51**, 392.
- 14 O. Petrovskaia, B. M. Taylor, D. B. Hauze, P. J. Carroll and M. M. Joullié, *J. Org. Chem.*, 2001, **66**, 7666.
- 15 Y.-I. Park, J.-H. Son, J.-S. Kang, S.-K. Kim, J.-H. Lee and J.-W. Park, *Chem. Commun.*, 2008, 2143.